

Flow behind a cylinder forced by a combination of oscillatory translational and rotational motions

M. Nazarinia, D. Lo Jacono,^{a)} M. C. Thompson, and J. Sheridan

Department of Mechanical and Aerospace Engineering, Fluids Laboratory for Aeronautical and Industrial Research (FLAIR), Monash University, Melbourne, 3800 Victoria, Australia

(Received 3 February 2009; accepted 28 April 2009; published online 20 May 2009)

The flow behind a cylinder undergoing forced *combined* oscillatory motion has been studied. The motion consists of two independent oscillations: cross-stream translation and rotation. Previous studies have extensively investigated the effect of these motions individually on cylinder wakes; however, the investigation of their combined effect is new. The motivation lies in its application to vortex-induced vibration and its suppression and to biomimetic motion. The focus is on the effect of the phase difference between the two motions. The results show that there is an unexpected loss of synchronization of the wake for a finite range of phase differences. © 2009 American Institute of Physics. [DOI: 10.1063/1.3139184]

The primary goal of this research is to understand the physical mechanisms behind the response of a cylinder wake to the combined forcing mechanisms of cross-stream translation and rotational oscillations. With an in-depth understanding of the flow physics it may be possible to propose a novel means of actively or passively suppressing the lock-on between vortex shedding and transverse oscillation. Also, we are interested in the application to biomimetic motions and, in particular, to carangiform motion.¹ There has been considerable research on the effect of either transverse or rotational oscillations on cylinder wakes, as discussed in the extensive reviews.^{2,3} Primarily, these have focused on the translational oscillation due to their focus on vortex-induced vibration. There have also been studies of the effect of rotational oscillation on wakes.^{4,5} Previous numerical work has also been performed on the effect of the combined motions in quiescent fluids⁶ and when there is a flow past the cylinder;⁷ however, the influence of an important parameter was not considered. Indeed, previous interesting results^{6,8} indicate that the phase difference between the two motions is of considerable importance and this is the focus of the research discussed here. This work is part of a more extensive set of experiments that considers the full range of independent variables.

The experiments were conducted in the FLAIR free-surface closed-loop water channel at Monash University. A schematic of the problem is given in Fig. 1. The cylinder used was 800 mm in length and with an outer diameter of $D=20$ mm, giving an aspect ratio of 40. The experiments were performed for a fixed upstream velocity $U_\infty=0.0606$ m/s giving $Re=U_\infty D/\nu=1322$. Two sinusoidal motions were imposed, namely, translational (cross stream), given by $y(t)=A_t \sin(2\pi f_t t)/D$, and rotational, given by $\theta(t)=A_\theta \sin(2\pi f_\theta t + \Phi)$. The frequencies are fixed close to that of the natural frequency ($T^{-1}=f_t=f_\theta=0.6$ s⁻¹ $\approx f_N$). The natural frequency was found to be equal to $f_N \approx 0.6154$ s⁻¹.

The Strouhal number based on this frequency is about $St \approx f_N D/U_\infty=0.203$ and the Strouhal number of the forcing is $St_f \approx f_t D/U_\infty=0.198$. The experiments presented are for fixed amplitudes of oscillation, $A_t=D/2$ and $A_\theta=1$. These amplitudes combined with the equal frequencies provide equal maximum velocities from the translational and rotational motions. The maximum velocities from the forcing are equal to $U_{\max}=2\pi f_t A_t=0.0377$ m/s which correspond to a ratio of $U_{\max}/U_\infty=0.62$.

As mentioned earlier, the results presented here show the effect of the phase difference (Φ) between the translational and rotational motions on the wake. This parameter was chosen as its variation led to interesting behavior in a *quiescent* fluid. Only a brief outline of that case will be given; a more detailed discussion can be found in Refs. 1 and 6. If the maximum velocities of the oscillatory motions are equal, it can easily be shown that there will be an uneven distribution of velocity at the surface of the cylinder depending on the phase imposed. Indeed, for opposing phases ($\Phi=180^\circ$) the two velocities will cancel on one side (orthogonal to the translational motion) and add on the other side. This creates a vorticity difference between the two halves of the cylinder, resulting in a wake flow orthogonal to the translational movement. The method used here to characterize the wake of this forced cylinder is via particle image velocimetry (PIV). The flow was seeded with spherical granular polyamide particles having a mean diameter of 55 μm and specific gravity of 1.016. The particles were illuminated using two mini yttrium aluminum garnet laser sources. The plane of interest for these experiments was orthogonal to the cylinder's axis (xy plane) and downstream (x direction) of the cylinder. A small section of the cylinder is replaced by a thin-walled transparent cylinder, whose interior is filled with distilled water. It is located at about $9D$ from the end of cylinder. The measured xy plane is located through the center of this window. The experimental setup provided a field of view of approximately $6D \times 6D$.

Figure 2 presents motion phase-locked vorticity isocontours taken at $t=T$ for various phase differences. The image

^{a)}Electronic mail: david.lojacono@eng.monash.edu.au.

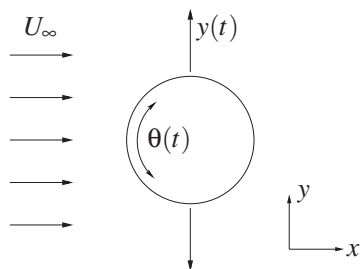


FIG. 1. Schematic showing the problem geometry and important parameters relevant to the combined forced oscillation and the circular cylinder model. The streamwise direction is the x direction.

at the top left shows the case where the two motions are of opposite phase ($\Phi = 180^\circ$); we observe a $2S$ mode (two single vortices shed per period) in a single row aligned in the medial plane. The field of view does not allow us to see the double row that should occur further downstream.^{9–11} The structure of a double-row wake is shown for the $\Phi = -30^\circ$ case, in which alternate vortices align in two rows offset from the centerline. As the phase difference is reduced toward being in phase, $\Phi = 30^\circ$, the vortices are arranged closer to each other and are less well aligned with the medial plane, suggesting an earlier double-row transition. The in-phase case, $\Phi = 0^\circ$, presents the signature of a $P+S$ mode (a single vortex and a vortex pair formed per cycle), at least in the near wake. The classification of the different vortex modes is given in Ref. 12. For this in-phase case, the vortices are shed widely apart (nearly $4D$), readily explained by the rotational oscillation adding momentum to the translational motion. The resulting strain favors a transition to the $P+S$ wake.¹³ Reducing the phase difference to $\Phi = -30^\circ$ and $\Phi = -60^\circ$, the vorticity pattern returns to a $2S$ mode in a double-row configuration. It should be noted that the spacing between the two rows reduces (from $2.5D$ to $2D$) as we decrease Φ . The cases of $\Phi = -90^\circ$ and $\Phi = -120^\circ$ are of particular interest:

Contrary to the other experimental cases, these two cases were not synchronized with the translational motion beyond $2D$ downstream. The effect of this loss of synchronization can be seen in the rapid downstream dissipation of the mean vortex structures due to averaging. Only the two vortices near the cylinder remain coherent. This *a priori* surprising phenomenon might be explained by the fact that the separation between the two rows of vortices is smaller and that this arrangement of vortices is not stable. Similar behavior can be found behind elliptical cylinders.¹¹ The last case $\Phi = -150^\circ$ (and necessarily the first case, $\Phi = \pm 180^\circ$) displays vortices in a single row.

In addition to the experiments, numerical simulations have been undertaken to elucidate certain behavior and to confirm certain aspects of the unlocked regime. Although these (two-dimensional) numerical simulations are performed at a much lower Reynolds number, the near-wake predictions are predominantly consistent with the experimental results (e.g., the vorticity pattern). This is likely due to the strong forcing, partially overriding the modifying effect of three-dimensional transition, at least for the near wake.

The description of the numerical methodology will be brief because it has been adequately described in previous papers. Details of the general method and its implementation can be found elsewhere.^{14,15} The code employed has been well proven for use in bluff-body problems.^{16–18} The time-asymptotic wake flows for the present study were calculated by solving the incompressible, time-dependent Navier–Stokes equations in a translating accelerating frame of reference attached to the cylinder. The discretization method employed was a spectral-element method using seventh-order Lagrange polynomials associated with Gauss–Lobatto–Legendre quadrature points. The computational domain, consisting of a semicircular upstream section and a rectangular downstream section, extended at least $30D$ in all directions. This was split into 518 elements, the majority of which were

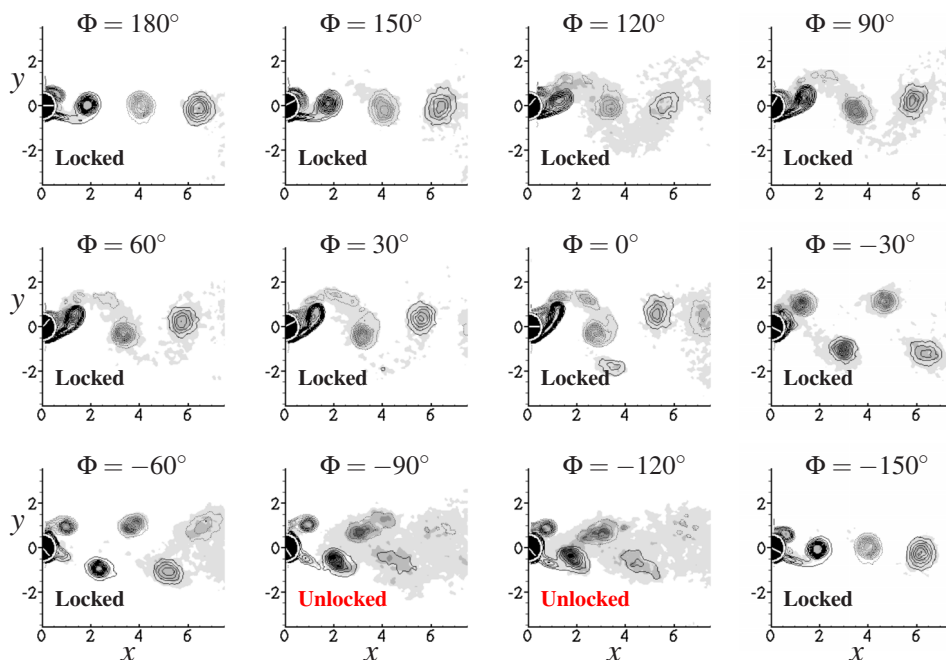


FIG. 2. (Color online) Motion phased-locked vorticity isocontours (lines) and root mean square vorticity (gray-scale) taken at the motion phase $t=T$. The near-wake vorticity is shown for different phase differences between the two imposed oscillatory motions. Of particular interest is the asynchronous (unlocked) wake with the imposed translational motion for the phases $\Phi = -90^\circ$ and $\Phi = -120^\circ$.

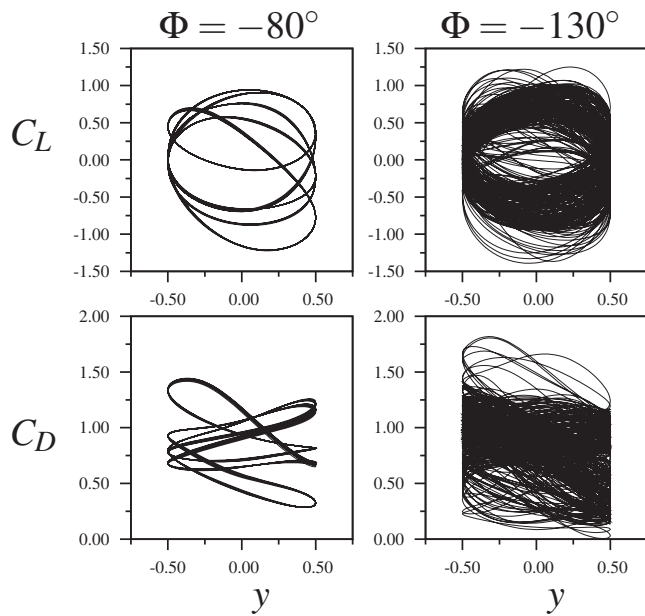


FIG. 3. Lissajous pattern defined horizontally with the translational forcing mechanism (y) and vertically with lift (top) or drag (bottom) coefficient.

concentrated in the cylinder boundary layer and wake regions. At the cylinder surface, a time-dependent Dirichlet condition was used that varied sinusoidally in time according to the driven rotational oscillation. In all cases the numerical simulations were performed for more than 200 cycles and started at rest. This was found to be sufficient for the asymptotic state to be achieved.

Various methods were used to analyze and characterize the predictions. Lissajous figures of the lift and drag coefficients against the transverse forcing mechanism for each phase difference have been produced. From these one can assess whether the flow was periodic, quasiperiodic, or highly irregular (or chaotic). Examples for two different cases are given in Fig. 3. The left-hand figures show *quasi-periodic* behavior with the phase plots repeating after five forcing periods. The right-hand figures indicate chaotic behavior since the trajectories do not repeat.

Some representative base flows are displayed in Fig. 4. Despite the Reynolds number difference (simulations $Re = 225$, experiments $Re = 1322$) these qualitatively reproduce the near-wake behavior of the PIV results. For $\Phi > -20^\circ$ a single row of vortices is displayed. For $-30^\circ \leq \Phi \leq -20^\circ$ a double row of vortices appears after a single row of vortices. The number of vortices in a single row diminishes as we approach $\Phi = -30^\circ$. For $-70^\circ \leq \Phi \leq -30^\circ$, the wake no longer displays an initial single row but instead immediately forms a double row. These vortex rows interact further downstream to form a quasiperiodic far wake. The number of vortices forming the double row diminishes as Φ diminishes. For $-130^\circ \leq \Phi \leq -80^\circ$ the wake immediately transitions to a fully chaotic state. For $\Phi < -130^\circ$ the flow undergoes a succession of double row, to single row, then double row, until a unique single row pattern. See the top wake pattern of Fig. 4 as representative of this final case.

Table I reports the experimental and numerical behaviors

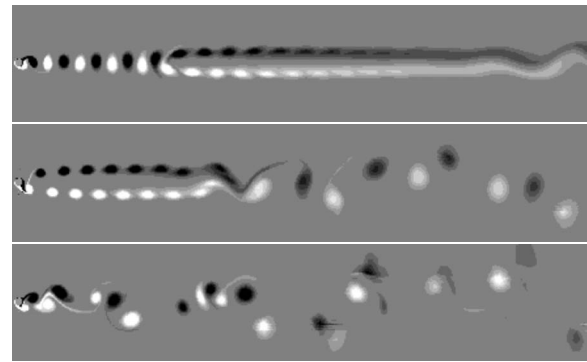


FIG. 4. Typical flow features for different imposed phase differences. Top: single row of vortices transitioning downstream to a double row followed by a further secondary instability in the far wake ($\Phi = -170^\circ$). Center: double row of vortices followed by a quasiperiodic pattern ($\Phi = -40^\circ$). Bottom: chaotic pattern of vortices ($\Phi = -100^\circ$). The domain of the numerical simulation was extended to $100D$ downstream for these cases.

of the wake flow for the same set of parameters *but* with $Re = 225$ for the numerical results. As we will see the discrepancy in the value of the Reynolds number does not have an impact on the synchronization for Φ values close to the loss of synchronization. The numerical simulations confirm the loss of synchronization for qualitatively the same region as the experiments. The numerical simulations reveal that the unlocked regime contains quasiperiodic and chaotic patterns. It appears that the chaotic regime is surrounded by quasiperiodicity. Also the likelihood of an unlocked regime is greater when the ratio f_i/f_{st} is higher than unity.

TABLE I. Summary of the synchronization around the unlocked regime. L, QP, and C stand for locked on, quasiperiodic, and chaotic, respectively. The unlocked regimes (UL) for the experimental results are likely to be chaotic. f_i and f_{st} stand for forced frequency and natural frequency for a fixed cylinder.

Φ (deg)	Expt. ≈ 1	f_i/f_{st}		
		Numerical		
		0.9	1.0	1.1
-30	L	L	L	L
-40		QP	L	L
-50		QP	L	QP
-60	L	QP	QP	QP
-70	UL	QP	QP	C
-80	UL	QP	QP	C
-90	UL	QP	C	C
-100	UL	QP	C	C
-110	UL	L	C	C
-120	UL	L	C	C
-130		L	C	C
-140		L	QP	C
-150	L	L	L	C
-160		L	L	L
-170		L	L	L
-180	L	L	L	L

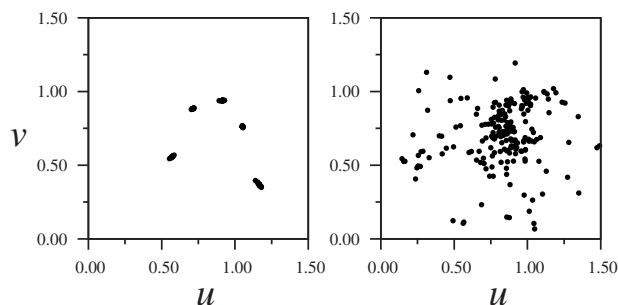


FIG. 5. Poincaré map for two typical unlocked regimes for $Re=225$. Left: quasiperiodic behavior for $\Phi=-80^\circ$. Right: chaotic regime for $\Phi=-130^\circ$. The phase diagram shows the horizontal and the vertical velocities at $7D$ downstream on the centerline.

To further examine the behavior, Poincaré maps have been constructed for each phase difference. The horizontal and vertical velocities are sampled at a prechosen point downstream, $(x, y) = (7D, 0)$, at the end of each forcing period T . For example, Fig. 5 illustrates the quasiperiodicity of the case where $\Phi = -80^\circ$. Here the periodicity of the flow is of $5T$ as can be seen from the distribution of five distinct islands of points in the phase diagram. The chaotic nature of the regime in the case of $\Phi = -130^\circ$ can be readily seen by inspection, with the distribution of points in the phase diagram showing no preferred region or cycle.

It appears that *synchronization* may not be a clear concept. Both the experimental and numerical results show that the size of the nearly periodic near-wake region is very much a function of the phase difference. Both sets of results show that this section of the wake becomes very short for $\Phi \approx -100^\circ$. Further downstream the wake undergoes a rapid transition to a chaotic state. For other phase difference ranges, the ordered near-wake persists further downstream but still can be subject to secondary transitions resulting in a quasiperiodic or chaotic far wake. If one measures the wake response using integral measures such as the lift or drag coefficient, then these will be affected to some extent by the far-wake behavior, even though they primarily respond to the wake state near the cylinder. If the ordered near-wake region is long, then these global measures should indicate synchronization. As the near-wake is reduced in length, the far-wake behavior can influence the signal recorded at the cylinder so that it contains low frequency components or even increases the frequency content to such an extent that the behavior is chaotic. Interestingly, quasiperiodic and chaotic far-wake behaviors can be observed for elliptical shaped cylinders¹¹ and the normal flat plate,¹⁹ even in the unforced case.

Experiments and numerical simulations (not shown here) suggest that the suppression mechanism also holds for smaller amplitudes of motion (A_θ and A_x). For the first time experiments have been carried out on a cylinder wake when the cylinder is experiencing combined rotary and transla-

tional oscillations. The effect of the phase differences between the two forced motions reveals that regular shedding can be suppressed for particular phase differences. This experimental study raised interesting features that were interpreted with the aid of numerical simulations, which qualitatively capture the near-wake behavior.

M.N. would like to acknowledge the support of a Monash Graduate Scholarship (MGS) and Monash International Postgraduate Research Scholarship (MIPRS). D.L. acknowledges support from ARC Discovery Grant No. DP0774525 and the Australian Partnership for Advanced Computing (APAC). We are also grateful to Alexis Cuquel for having helped with the numerical simulations.

- ¹H. M. Blackburn, J. R. Elston, and J. Sheridan, "Bluff-body propulsion by combined rotary and translational oscillation," *Phys. Fluids* **11**, 4 (1999).
- ²C. H. K. Williamson and R. Govardhan, "Vortex-induced vibration," *Annu. Rev. Fluid Mech.* **36**, 413 (2004).
- ³T. Sarpkaya, "A critical review of the intrinsic nature of vortex-induced vibrations," *J. Fluids Struct.* **19**, 389 (2004).
- ⁴P. T. Tokumaru and P. E. Dimotakis, "Rotary oscillation control of a cylinder wake," *J. Fluid Mech.* **224**, 77 (1991).
- ⁵J. R. Filler, P. L. Marston, and W. C. Mih, "Response of the shear layers separating from a circular cylinder to small amplitude rotational oscillations," *J. Fluid Mech.* **231**, 481 (1991).
- ⁶J. R. Elston, "The structures and instabilities of flow generated by an oscillating circular cylinder," Ph.D. thesis, Monash University, 2006.
- ⁷S. Kocabiyik and Q. M. Al-Mdallal, "Bluff-body flow created by combined rotary and translational oscillation," in *Fluid Structure Interaction and Moving Boundary Problems*, WIT Transactions on the Built Environment, Vol. 84, edited by S. Chakrabarti (WIT, Southampton, UK, 2005), p. 195.
- ⁸J. S. Leontini, B. E. Stewart, M. C. Thompson, and K. Hourigan, "Predicting vortex-induced vibration from driven oscillation results," *Appl. Math. Model.* **30**, 1096 (2006).
- ⁹H. Lamb, *Hydrodynamics* (Dover, New York, 1932).
- ¹⁰J. M. Cimbala, H. M. Nagib, and A. Roshko, "Large structure in the far wakes of two-dimensional bluff bodies," *J. Fluid Mech.* **190**, 265 (1988).
- ¹¹S. A. Johnson, M. C. Thompson, and K. Hourigan, "Predicted low frequency structures in the wake of elliptical cylinders," *Eur. J. Mech. B/Fluids* **23**, 229 (2004).
- ¹²C. H. K. Williamson and A. Roshko, "Vortex formation in the wake of an oscillating cylinder," *J. Fluids Struct.* **2**, 355 (1988).
- ¹³J. S. Leontini, B. E. Stewart, M. C. Thompson, and K. Hourigan, "Wake state and energy transitions of an oscillating cylinder at low Reynolds number," *Phys. Fluids* **18**, 067101 (2006).
- ¹⁴G. E. Karniadakis and S. J. Sherwin, *Spectral/hp Methods for Computational Fluid Dynamics* (Oxford University Press, Oxford, 2005).
- ¹⁵M. C. Thompson, K. Hourigan, and J. Sheridan, "Three-dimensional instabilities in the wake of a circular cylinder," *Exp. Therm. Fluid Sci.* **12**, 190 (1996).
- ¹⁶K. Ryan, M. C. Thompson, and K. Hourigan, "Three-dimensional transition in the wake of bluff elongated cylinders," *J. Fluid Mech.* **538**, 1 (2005).
- ¹⁷J. S. Leontini, M. C. Thompson, and K. Hourigan, "Three-dimensional transition in the wake of a transversely oscillating cylinder," *J. Fluid Mech.* **577**, 79 (2007).
- ¹⁸D. Lo Jacono, J. N. Sørensen, M. C. Thompson, and K. Hourigan, "Control of vortex breakdown in a closed cylinder with a small rotating rod," *J. Fluids Struct.* **24**, 1278 (2008).
- ¹⁹F. M. Najjar and S. Balachandar, "Low-frequency unsteadiness in the wake of a normal flat plate," *J. Fluid Mech.* **370**, 101 (1998).